

Model Validation and Performance Assessment of Unglazed Photovoltaic-Thermal Collectors with Heat Pump Systems

Bharat Chhugani, Peter Pärtsch, Maik Kirchner, Matthias Littwin,
Carsten Lampe and Federico Giovannetti

Institute for Solar Energy Research Hamelin (ISFH), 31860 Emmerthal (Germany)

Abstract

PVT collectors convert solar radiation into both useful heat and electricity. Therefore, with the same PV area more solar energy could be harvested. The work investigates a novel unglazed liquid-based PVT collectors as a single source in a heat pump system for the energy supply of a single-family house. In this hybrid collector, the PV panel is thermally coupled with a specially designed brine-to-air heat exchanger on backside, which enables to gain energy from the sun and ambient air. Therefore, this novel collector is validated with the PVT collector model in TRNSYS for varying weather conditions based on the measurement results from our test facility and presented in the paper. The comparison shows good agreement, despite the missing reproduction of icing and detailed condensation processes in the simulation type. Based on this model, the impact of a PVT-heat pump system is further investigated by yearly dynamic simulations in TRNSYS for space heating, domestic hot water and defrosting of PVT. The results show that the seasonal performance factor of the PVT to HP system can reach 3.18 with the PVT area of only 20 m². The seasonal performance factor including self-consumed PV fraction for the heating system reaches 3.49 with the same collector area and without any additional battery storage.

Keywords: Photovoltaic-Thermal (PVT) collector, TRNSYS Simulation, heat pump system

1. Introduction and methodology

Photovoltaic - Thermal (PVT) collectors are a combination of a solar thermal collector and a photovoltaic module in a single component, which simultaneously generates power and heat from the same area. Therefore, PVT can maximise the fraction of renewable energy source utilisation. Nowadays, commonly available liquid-based PVT collectors are unglazed PVT collector (WISC), glazed PVT collector, concentrating PVT collector (CPVT) (Lämmle 2018). Unglazed PVT collectors are beneficial for operation near ambient temperatures particularly because of high heat transfer to ambient air even in times of low radiation (Lämmle 2018). Among all three collector types, unglazed PVT collectors are widely popular in the northern European market also as an additional heat source for heat pumps (Bertram et al. 2011; Hüsing et al. 2018).

In the presented research work, unglazed SOLINK PVT collectors have been comprehensively investigated. This PVT collector concept has been developed by the company Consolar Solare Energiesysteme GmbH, Karlsruhe Institute of Technology (KIT), and Triple Solar B.V. (Leibfried et al. 2017) and is shown in Figure 1. The PVT collector is thermally coupled with a fin-tube heat exchanger on the backside of PV. The fin surface area is 10 times larger than the PV area in each module, which increases the use of energy from the sun and ambient air and hence the PVT collector works as a good environmental heat exchanger. In addition to convective heat gains in times of low irradiation particularly in winters or nights, condensation heat gains, as well as heat gains through the phase change to frost occur on larger fins surfaces, which improves the thermal collector output and makes it suitable for working as a sole heat source of a heat pump. Therefore, this unglazed PVT offers a promising alternative to conventional geothermal sources of brine-water heat pumps as well as to an air-water heat pump.

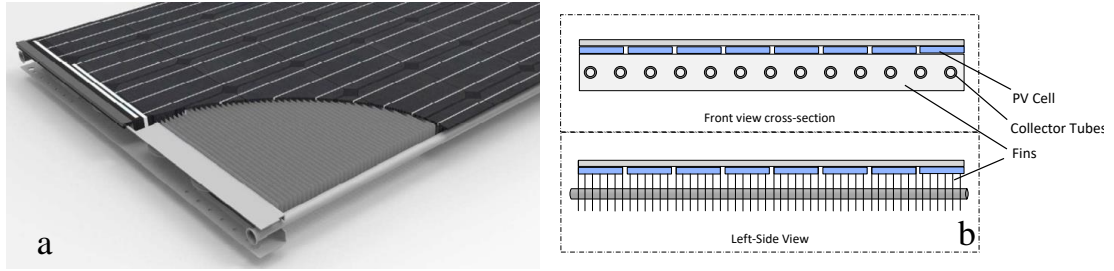


Fig. 1: (a) Sectional view of the PVT collector: the fin tube heat exchanger on the backside of the surface (Leibfried 2018), (b) Schematic diagram of PVT Collector

Within the scope of the research project “TwinPower”, nine south-facing PVT Modules with the area of $\sim 18 \text{ m}^2$ (in Figure 2 right) have been installed and monitored at the test roof of ISFH. Additionally, nine standard PV modules have also been monitored for the direct comparison of the electrical performance of thermally cooled PVT and non-cooled PV modules. The PV module field is shown in Figure 2 (left).



Fig. 2: Module test fields at the ISFH (left: PV module field; right: PVT field)

Both modules have identical PV cells, and their electrical characteristics under Standard Test Conditions (STC) are shown in table 2.

Tab. 1: Electrical characteristic data of the investigated PVT collector (STC)

Pmax (Wp)	Electrical Efficiency (η_{el})	Open circuit voltage (Voc)	Short circuit current (Isc)	Maximum power voltage (Vmp)	Maximum power current (Imp)	Power temperature coefficient
340 W	17.5 %	48.0 V	9.45 A	37.6 V	9.05 A	- 0.39 %/K

The thermal efficiency of this PVT collector was determined by means of outdoor measurements at IGTE (University of Stuttgart) according to the Standard ISO 9806:2013 as part of a Solar Keymark certification. Table 2 shows the thermal collector parameters for this single module test. Additional investigations of the collector have been carried out at ISFH and extensively presented in (Giovannetti et al. 2019; Lampe et al. 2019), The authors analysed the performance of a collector field under real environmental conditions. The correspondent results are presented in Table 3.

Tab. 2: Thermal collector parameter of single PVT module according to Solar Keymark Test (Giovannetti et al. 2019)

Thermal collector parameters (MPP)	
$\eta_{0,b}$ (collector efficiency)	0.468
c1 (heat loss coefficient in $\text{W/m}^2\text{K}$)	22.99
c3 (wind dependence heat loss coefficient in $\text{J/m}^3\text{K}$)	7.57
c4 (sky temperature dependence of the heat loss coefficient)	0.434
c5 (collector capacity in $\text{kJ/m}^2\text{K}$)	26.05
c6 (wind dependence conversion factor in s/m)	0.067

Additionally, a PVT heat pump system has also been investigated in a Hardware-in-the-Loop (HiL) real-time test environment. In HiL tests, the energy source (PVT collectors), the heat pump (HP) and the thermal buffer storage operate in real-time as hardware. A TRNSYS co-simulation calculates the space heating demand (SH) of the building and the test facility emulates the energy sinks for domestic hot water (DHW) and space heating (SH). Results of the HiL measurement are briefly presented in (Chhugani et al. 2020). The goal there was to analyse and evaluate the system for the energy supply of a single-family house under dynamic weather conditions. The results showed a good system efficiency (average daily performance factor 3.3) when PVT collectors are directly coupled with the heat pump as a sole heat source. According to these first tests, the PVT assisted HP could be a promising alternative to an air-source heat pump.

In the presented investigation, data from the PVT measurements have been used for validation of the TRNSYS type 203 (Stegmann. et al. 2011). Type 203 is based on parameters resulting from standard test procedures of the thermal and electrical characteristic curve. It was developed by ISFH and successfully validated for the use with ground-coupled heat pump systems. The new validation methodology is shown in Figure 3. The type calculates the simulated collector outlet temperature, thermal and electrical collector yield and the condensation gains. However, the condensation gains are only calculated from the front surface of the collector, which might lead to some uncertainty in case of SOLINK PVT collector because of its unique construction with fins on the rear side. The influence of icing, precipitation, and wind direction, which are expected to play a relevant role, can cause deviation in simulation output.

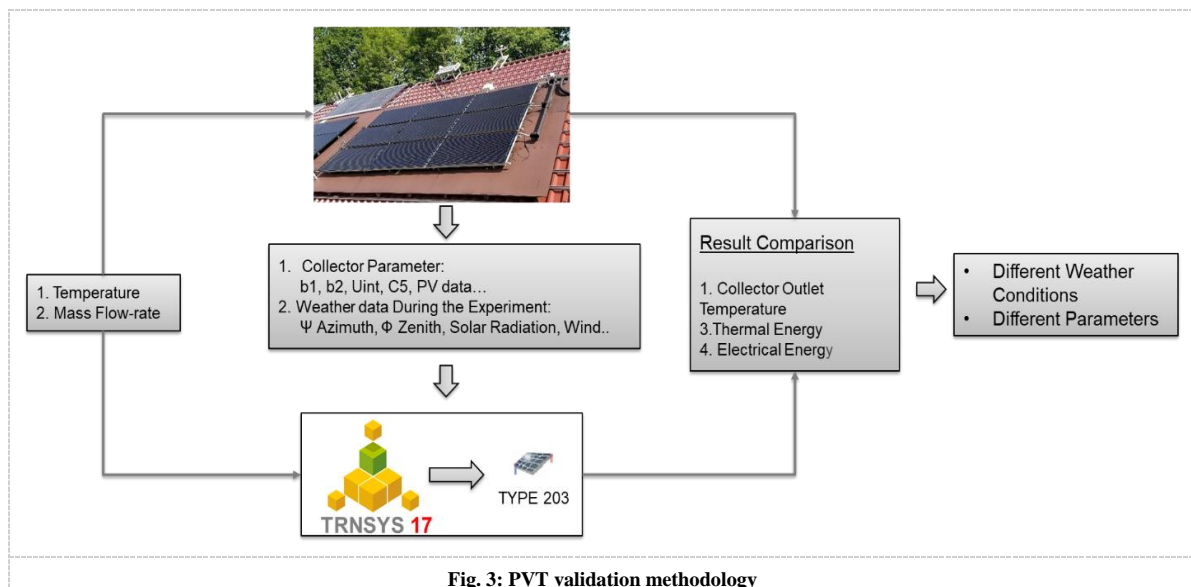


Fig. 3: PVT validation methodology

In order to validate the model, meteorological and energetic data of the collector are measured at ISFH with one-second time steps, which includes collector in- and outlet temperatures, flow rate, longwave irradiance, air velocity, global and diffuse irradiance, ambient air temperature, and humidity. In the end, all measured and calculated data are fed into the simulation and compared with real outputs. For the PVT validation, different collector parameter sets have been investigated. Firstly, the Solar Keymark parameters, which result from the single collector test. The second parameter set was determined from the PVT collector field test at ISFH, as explained in (Giovannetti et al. 2019; Lampe et al. 2019). Both parameter sets are summarised in Table 3. The results show that the overall heat transfer coefficient U -value ($U = c_1 + c_3 \cdot wind$) of the PVT field is reduced by about 20 % compared to the U -value determined from the single panel. The reduction is caused largely by the different wind exposure of the collector and the high sensitivity of the collector design (finned heat exchanger). Both parameter sets have been used in the simulation/validation and compared with measured outputs.

In contrast to the ISO 9806:2013, type 203 requires the thermal collector parameter determined according to the test standard EN 12975. Hence, the values of the Solar Keymark datasheet are converted according to the following equations (1 to 5). Table 3 also shows the performance parameters of an additional reference PVT

module, which was developed by ISFH and used for comparison with the SOLINK PVT in yearly system simulations (chapter 3).

$$c_1 = b_1 \quad (\text{eq. 1})$$

$$c_3 = b_2 \quad (\text{eq. 2})$$

$$c_4 = \eta_{0,\text{hem}} \cdot \frac{\varepsilon}{\alpha} \quad (\text{eq. 3})$$

$$c_6 = \eta_{0,\text{hem}} \cdot b_u \quad (\text{eq. 4})$$

$$\eta_{0,\text{hem}} = \eta_{0,b} \cdot K_b(\theta) \cdot \frac{G_b}{G} + \eta_{0,b} \cdot K_d \cdot \frac{G_b}{G} \quad (\text{eq. 5})$$

Where ε is hemispherical emittance, α is solar absorptance, G_b is direct solar irradiance for beam irradiance, K_d is incidence angle modifier for diffuse radiation, θ is the angle of incidence.

Tab. 3: Thermal collector parameters used in PVT validation and system simulation

Thermal Collector Parameters (MPP)	Solar Keymark Test Parameter	ISFH -Field Test Parameter	Reference PVT module (ISFH)
$\eta_{0,b}$ (Zero-loss efficiency based on beam irradiance)	0.468	0.532	0.661
b1 (Heat loss coefficient in W/m ² K)	22.99	19.08	12.47
b2 (Wind dependence heat loss coefficient in J/m ³ K)	7.57	3.69	3.71
bu (Wind dependence conversion factor in s/m)	0.144	0.126	0.079
collector capacity in kJ/m ² K	26.05	26.05	15.00

2. PVT model validation

2.1 Validation under winter conditions

In general, simulated and measured results of thermal energy output are expected to show good agreement because the simulation model uses the collector parameters determined from the collector tests. The first validation is performed for winter measurement with Solar Keymark test parameter over a total measuring period of 50 hours, from 7th to 9th January 2019 and is shown in Figure 4.

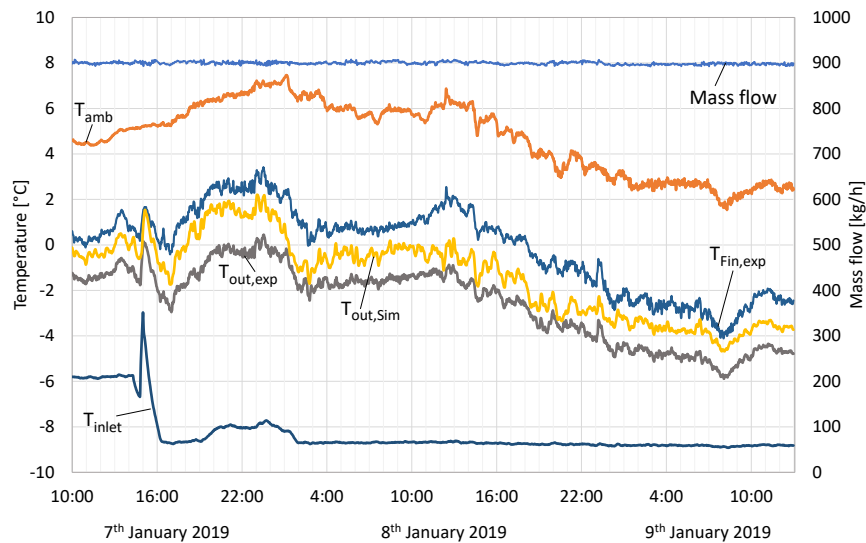


Fig. 4: Comparison of type 203 and measurements based on “Solar Keymark test parameters” for winter measurements

In Figure 4, the left axis shows ambient temperature (T_{amb}), collector inlet temperature (T_{inlet}), measured collector outlet temperature ($T_{out,exp}$), simulated collector outlet temperature ($T_{out,sim}$), measured collector fin temperature during the experiment ($T_{Fin,exp}$) and on the right axis mass flow rate in collector field. The results clearly show a significant deviation between the measured and simulated collector outlet temperature. The simulated outlet temperature is always higher than the measured output. Thus, the thermal performance, which is proportional to the temperature difference ($T_{out} - T_{inlet}$), is overestimated by the simulation model. This is caused by the higher heat loss coefficient exhibited by a single module compared to a larger collector field, due to the already mentioned different impact of ambient temperature and wind on the two configurations. In the PVT field, collectors are paced together, so that wind turbulence and velocity in the air gap between the roof and the field by nearby PVT modules are reduced. Both effects can be easily seen from table 3, where the value of b_2 from the field measurement is reduced by approx. factor 2 compared to the single module parameter and b_1 is roughly 20 % lower. Consequently, during the first validation attempt, the simulated thermal energy output was 20.2 % higher than the measured output over the considered time. Solar Keymark test parameters are thus not suitable to simulate PVT fields with SOLINK-collectors.

Further validation was performed by using the field test parameters. The simulation results are shown in Figure 5. The simulated outlet temperature shows good agreement with the measured value, and total thermal energy outputs during the considered time period were 14.8 kWh/m² simulated vs 15.8 kWh/m² measured. The slight deviation can be attributed to the following reasons: firstly, a wind direction effect on the heat loss coefficient because of the special finned heat exchanger of the SOLINK PVT. If the wind flows along the fin planes, the factor b_2 will increase and vice versa if the wind direction is perpendicular to the planes. Secondly, further disregarded meteorological influences, such as precipitation. Non-negligible thermal power can be exchanged between the unglazed solar collector and the rainwater. The rainwater temperature is very difficult to define according to climatic conditions, and this effect is comprehensively presented in (Bunea et al. 2015). And during the experiment, measured rainfall was 0.8, 10.7 and 0.3 litre/m² on 7th, 8th, 9th January respectively. Thirdly, missing condensation gains calculation from the backside of fins surface in the type. The condensation gains in type 203 are calculated only from the front side of the collector, and in the investigated field maximum condensation gains occur through the fins, which is not possible to simulate within this type. Condensation effect occurs if the surface temperature ($T_{Fin,exp}$) is below dew point and above frost point (between 0 °C to -3 °C). As fin temperature and dew point fall below the frost point, the correspondent heat transfer mechanism cannot be reproduced by the model as well.

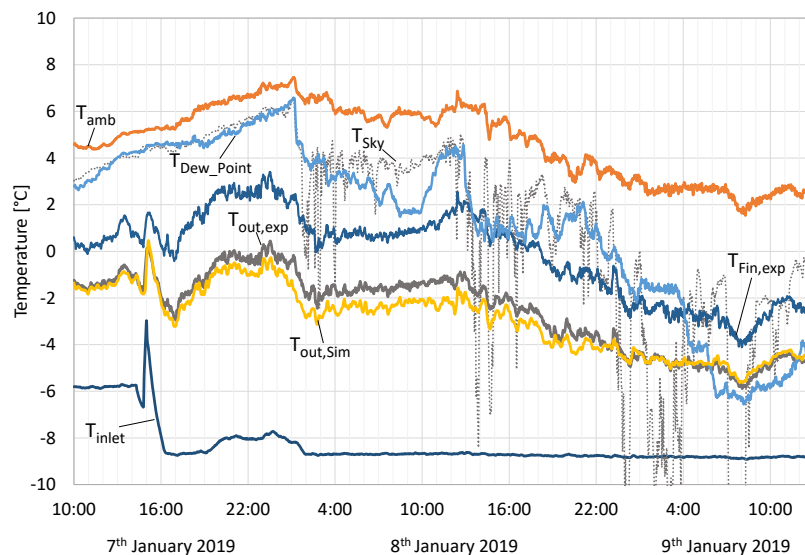


Fig. 5: Comparison of type 203 and measurements based on "ISFH - Field Test parameter" winter measurements

In the next phase, the PVT collector has been tested under frost and ice formation; the experiments and validations were carried out with PVT inlet temperatures below -10 °C for almost 34 hours. During the experiment, ice formation on the fins surface on the rear side of PVT was observed. Figure 6 shows this process

at three different times. The first picture shows the collector before ice formation, the second picture shows ice formation during the daytime, and the last one shows ice formation during nighttime. The timing of the respective pictures are represented with arrows in Figure 7, which displays the course of the relevant temperatures during experiments and simulations.



Fig. 6: Ice formation under the PVT collector field (back side of the PVT – fins surface)

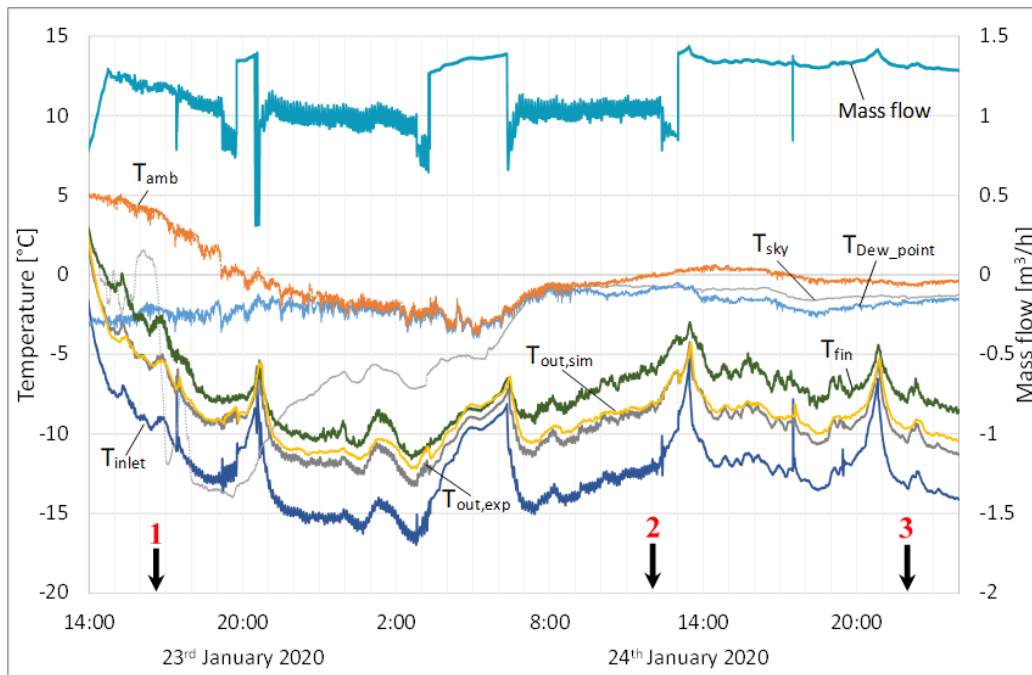


Fig. 7: Comparison of type 203 and measurements during ice formation on the PVT collector field

Quantitative comparison of simulations and measurement before ice formation (until arrow 1), shows only slight difference in thermal output (measurement: 0.87 kWh/m² vs simulation: 0.85 kWh/m²). After the ice formation on the collector (after point 1), stronger deviations are observed, and the simulated output is higher than measured values (measurement: 6.03 kWh/m² vs simulation: 7.12 kWh/m²). The most probable explanation for this deviation is an overestimation of convective gains (b_1 and b_2). The ice formation on the collector field is hindering the heat transport from ambient to the collector. On the other hand, the negative effect on heat loss because of the ice formation is not implemented in the model. However, this model error only occurs, when PVT is operating under extreme conditions (no defrosting of PVT, heat pump running continuously, no direct sunshine). Usually, this takes place only in few extreme winter days, and this is not the typical instance. In the simulation, this effect can be reduced by regularly defrosting of PVT collector, which is realistic and reduces the model errors. Therefore, in the yearly simulations PVT defrosting is also implemented.

2.2 Validation under summer conditions:

The type 203 has also been validated for summer weather conditions with using the ISFH field parameter set, over a total measuring period of 40 hours. The results are shown in Figure 8 (thermal output) and Figure 9 (electrical output). As illustrated in Figure 8, the measured thermal output is reproduced very well by the

model. However, the cooling energy during the night (02:00 to 06:00) shows some inconsistency, which is to some extent to be attributed to the special collector design and has to be addressed in future work for cooling applications.

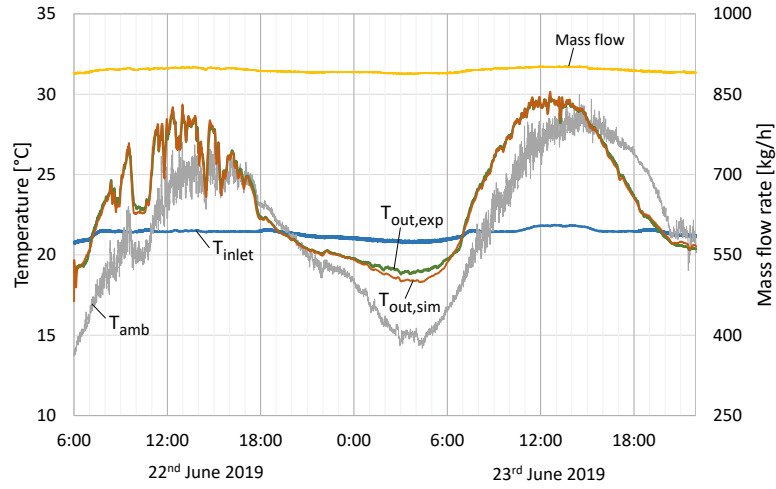


Fig. 8: Comparison of type 203 and measurements during summer measurements

During the same experiment, PVT electrical output from collectors is also compared with simulations. The electrical power shows excellent agreement with a deviation of approx. 2 %, the total electrical output measurement 2.38 kWh/m² to simulation 2.34 kWh/m². The slight difference between simulation and experiment power might be affected by the different estimation of the cell temperature because of the additional collector passive cooling with fins in the PVT field, which is not considered by the model.

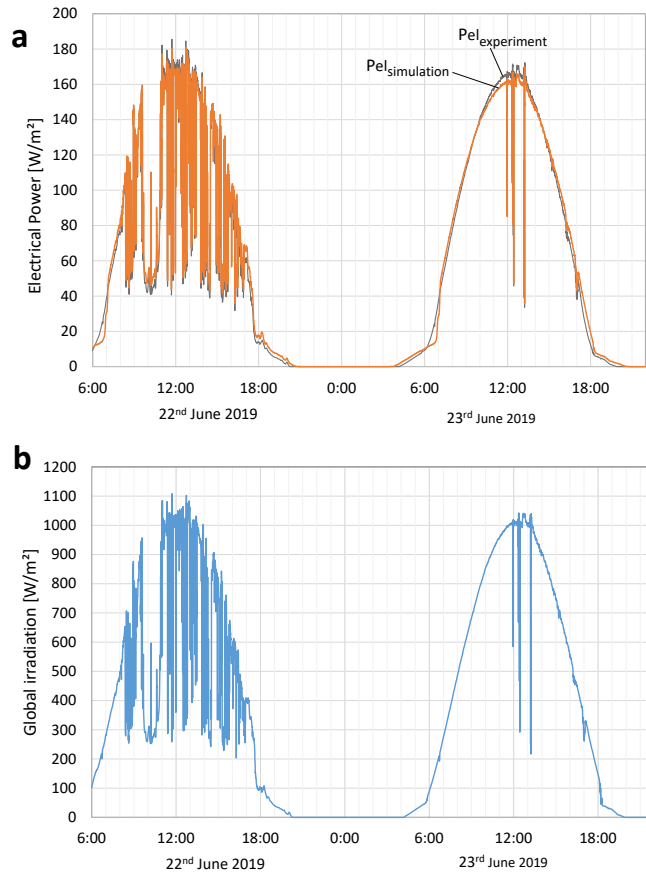


Fig. 9: Validation of type 203: (a) Electrical output during summer measurements (b) Measured global radiation near the collector plane

To conclude, it can be assumed that the simulation with type 203 model works well even for the SOLINK collector if collector parameter set from the field measurement is used. Besides, it is also expected that type 203 can be used in simulations with PVT coupled heat pump systems if icing and condensation gains do not play a relevant role during operation. For a more general implementation, the existing model needs to be extended in order to reproduce these additional effects. In the following section, the influence of the PVT on the heat pump system is explained by means of yearly simulations.

3. System simulation

PVT coupled HP system has been simulated with the dynamic simulation software TRNSYS (Transient System Simulation Program) to calculate the energy supply of a single-family house. Figure 10 illustrates the simulated thermal and electrical system. The system consists of PVT-modules as a sole heat source of the heat pump, thermal buffer storage at the sink side for domestic hot water preparation via instantaneous water heater and for space heating of the building. To avoid ice formation on/under the PVT field, a defrosting function is implemented in the yearly simulations, and the necessary heat is directly supplied by the storage via an external heat exchanger. The PVT-system with a DC/AC-inverter supplies electric energy to the heat pump system at first priority.

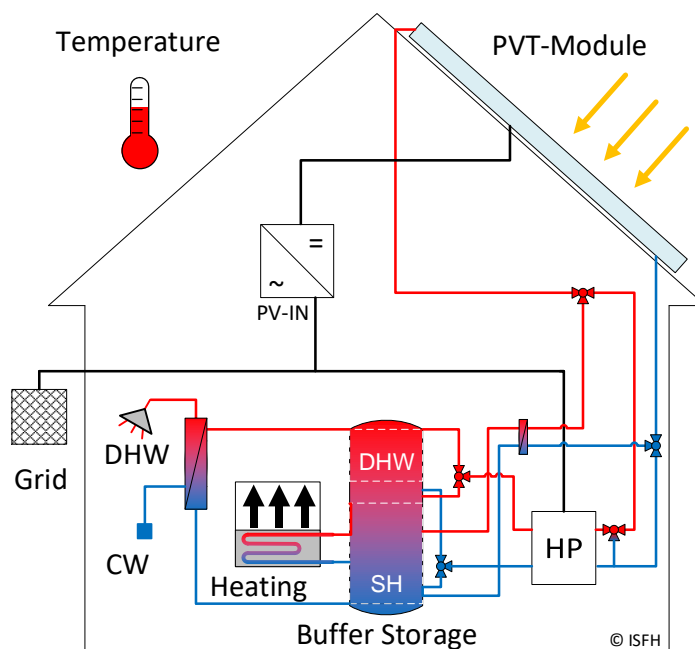


Fig. 10: Simulation system overview

The building model used in the investigations is the Single Family House (SFH45) based on IEA SHC, Task 44 / HPP Annex 38. The detailed description of the boundary conditions, load profiles and building components have been published within IEA Task 44 (Dott et al. 2013; Haller et al. 2013). SFH45 was developed in such a way that it can represent the heat demand and hot water demand of a new building with a good thermal insulated building envelope. An overview of the main simulation parameters is presented in Table 4. The tapping profile has been derived from DIN EN 16147 with an energy demand of approx. 5.8 kWh/d. The total flow of 145 litres/d with an average cold-water temperature of 10 °C is assumed and hot water is tapped at 45 °C. The required amount of heat for defrosting depends on the PVT design. Defrosting heat is taken from the storage via a heat exchanger, which increases the energy demand of the system. The defrosting demand was approx. 390 kWh/a for the collector field (PVT area 20 m²).

In the simulation, a brine-water inverter heat pump (HP) has been used with thermal power of 9.1 kW and the COP of 4.13 by B0/W35 at 75 % of compressor speed. This heat pump has been designed to operate with PVT collectors as a single heat source for low-temperature heating systems; therefore, the heat pump can work down to the minimum inlet temperature of -15 °C and maximum of 30 °C at the evaporator side. Moreover, the heat

pump has a backup electrical heater of 8 kW. For modelling TRNSYS type 401 was used.

Tab. 4. Description of the main simulation parameters

Description	Value
Location	Zurich (Switzerland)
Building size	140 m ² (Floor area)
Heat demand for space heating	SFH45 ≈ 48 kWh/(m ² ·a) (Floor heating)
Domestic hot water demand	2141 kWh/a (at 45 °C)
PVT collector (type 203)	1 m ² to 60 m ²
Thermal storage tank (type 340)	560 liter
T ambient average	9.9 °C
Irradiation on collector (diff + dir)	1276 kWh/(m ² ·a)

For the evaluation of the system, the seasonal performance factors (SPF) with different system boundaries have been used. These indicators are explained below in eq. 6 to 8 together with the square view (Figure 11).

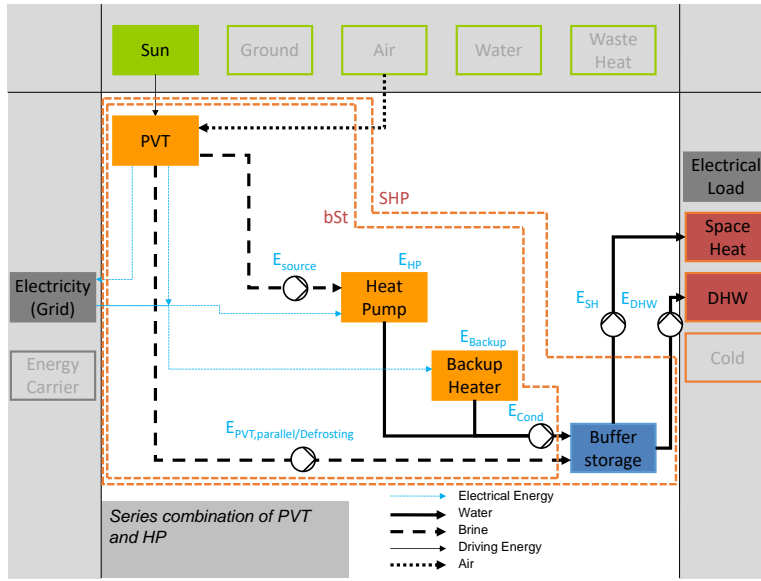


Fig. 11: System square view with different system boundary

First indicator SPF_{bSt} (before storage), is the ratio between amounts of heat supplied by the condenser ($\dot{Q}_{Condenser}$), backup heater (\dot{Q}_{Aux}) and energy delivered for defrosting and PVT direct loading energy ($\dot{Q}_{Defrosting/PVT,parallel}$) divided by the electrical energy provided within this boundary. \dot{E}_{HP} is electrical energy of the heat pump compressor, $\dot{E}_{source+Cond}$ is pumps energy of the source and sink side, \dot{E}_{Aux} is heater electrical energy and $\dot{E}_{PVT,parallel}$ is pump energy for defrosting or PVT direct.

The second indicator is the SPF_{SHP} of the system. It defines the ratio between amounts of heat delivered by the system (SH, DHW) to the electrical energy consumed over a specified period. Moreover, to make a system comparable with other systems, in SHP boundary, the electrical consumption of the heating and the water circulation pump of the building is not included in the system calculation. The index is defined according to IEA Task - 44 SHP boundary conditions (Malenković et al. 2012). In contrast to the SPF_{SHP} boundary, the next performance indicator $SPF_{SHP}^{(Grid)}$ represents self-consumed PVT electricity in SHP boundary (without battery storage) and is explained in eq. 8.

$$SPF_{bSt} = \frac{\int (\dot{Q}_{Condenser} + \dot{Q}_{Aux} + \dot{Q}_{Defrosting/PVT,parallel}) dt}{\int (\dot{E}_{HP} + \dot{E}_{source+Cond} + \dot{E}_{Aux} + \dot{E}_{PVT,parallel}) dt} \quad (eq. 6)$$

$$SPF_{SHP} = \frac{\int (\dot{Q}_{SH} + \dot{Q}_{DHW}) dt}{\int (\dot{E}_{HP} + \dot{E}_{source+Cond} + \dot{E}_{Aux} + \dot{E}_{PVT,parallel}) dt} \quad (eq. 7)$$

$$SPF_{SHP}^{(Grid)} = \frac{\int (\dot{Q}_{SH} + \dot{Q}_{DHW}) dt}{\int (\dot{E}_{HP} + \dot{E}_{source+Cond} + \dot{E}_{Aux} + \dot{E}_{PVT,parallel} - \dot{E}_{PVT}) dt} \quad (eq. 8)$$

In order to investigate the impact of PVT on system performance, two different PVT collectors have been compared: the SOLINK collector (field parameter set) and a reference PVT collector (Table 3). As the heat pump plays a crucial role in PVT coupled heat pump systems, especially when PVT has been designed to be used as a single heat source; therefore two different bivalence temperatures for the heat pump have been simulated. The bivalence temperature of a heat pump indicates that if the evaporator inlet temperature drops below the threshold, the electric heater is turned on, and the heat pump compressor stops. In the simulation, bivalence temperatures $-15\text{ }^{\circ}\text{C}$ and $-10\text{ }^{\circ}\text{C}$ were used. The bivalence temperature variations give an idea of the importance of selecting a proper heat pump because commonly market available heat pumps have a bivalence point up to $-10\text{ }^{\circ}\text{C}$.

Figure 12 illustrates seasonal performance factors depending on the different collector area. For the SOLINK PVT with an area of 20 m^2 and an inverter heat pump (bivalence of $-15\text{ }^{\circ}\text{C}$), the achieved SPF_{SHP} is 3.18. To achieve the same performance factor with the reference PVT collector, almost 30 m^2 PVT area is required.

On the other hand, with same collector but commonly available heat pump (bivalence of $-10\text{ }^{\circ}\text{C}$), the seasonal performance factor of the system decreases significantly, which is due to the additional use of an auxiliary heater. Approx. 40 m^2 of SOLINK PVT collector is required to reach SPF_{SHP} of 3.18, and with the reference PVT even 50 m^2 area is not enough to get the SPF of more than 3.1.

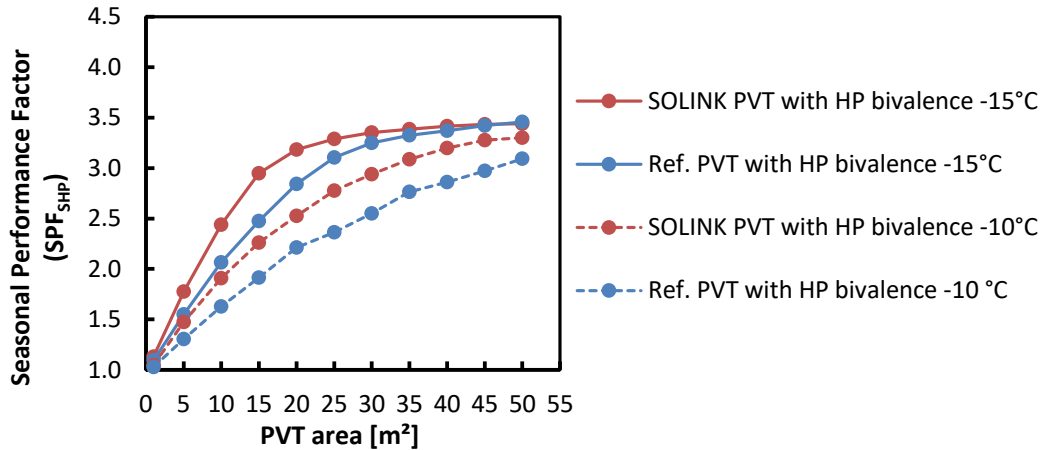


Fig. 12: Seasonal performance factor (SHP) as a function of the PVT collector area from 1 to 50 m^2 , for two different collectors and different bivalence points of the heat pump

Often PVT manufacturers tend to use the system performance factor including self-consumed PV electrical energy ($SPF_{SHP}^{(grid)}$). However, one has to pay attention to the priority of electricity consumptions, the household electricity profile or heat pump or the control strategy. Furthermore, this performance factor gives the PV electricity the same weightage as the electricity demand, which is not valid due to feed-in tariffs. In our case the $SPF_{SHP}^{(grid)}$ amounts to 3.49 with same 20 m^2 and increases gradually with the PVT area. No battery

storage and no household electrical consumption are considered. Figure 13 compares the three different performance factors.

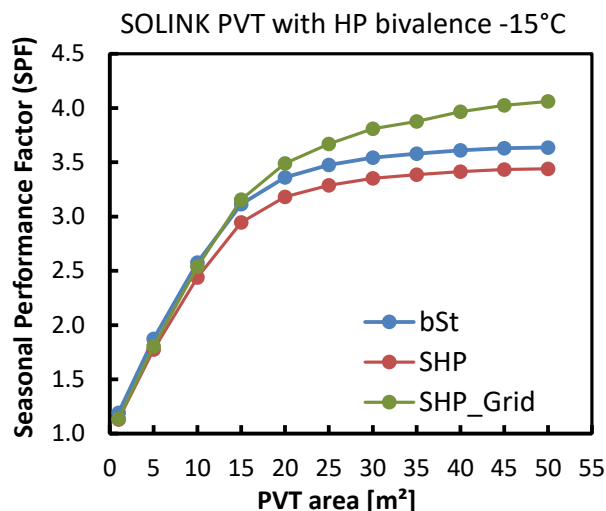


Fig. 13: Overview of three different Seasonal performance factor with the variation of the SOLINK PVT area from 1 to 50 m²

4. Conclusion

In the frame of a research project, investigations have been carried out on the SOLINK PVT collector with finned tube heat exchanger by means of experiments and simulations. The special construction of the PVT increases the convective heat transfer from the environment, and thus the collector acts as an excellent environmental heat exchanger. In the investigation, the PVT model type 203 is compared in TRNSYS with the measurement data. The result shows a very good agreement with collector parameters determined from field measurement at ISFH. The deviation is caused by the special design of the PVT with fins, which enhances convective heat transfer and condensation gains as well as by ice formation, which is not considered by the model and requires further development. Based on this model, PVT assisted heat supply systems have been investigated in TRNSYS for the energy supply of the single-family house (SFH45).

With the help of yearly system simulations, two main effects have been identified: efficient PVT panels (in our case SOLINK) can significantly improve the system performances and require fewer PVT panels compared to the reference PVT to get the same SPF. With the PVT area of 20 m², seasonal performance factors SPF_{SHP} and $SPF_{SHP}^{(Grid)}$ of 3.18 and 3.49 were achieved respectively for the location Zurich with cold winters and warm summers. In the assessment of PVT for heat pumps, much better results can be achieved by selecting an appropriate heat pump. In our case a lower bivalence temperature from -10 °C to -15 °C, can reduce the required PVT area by 50 % from 40 m² to 20 m², to get the same SPF.

Overall, when the investigated PVT collectors are directly coupled with the heat pump as a sole heat source, the achieved system efficiency is good and can be used as an alternative to an air source heat pump. Besides, by considering PV electrical generation (self-consumed), the system performance factor can be significantly increased. Moreover, in the simulation, the system has been investigated with a simple, demand-oriented system control strategy, and by changing to a more complex, PV oriented control strategy higher performance is expected.

5. Acknowledgements

The presented work and the results are part of the research project “TwinPower - 0325867B” and “integraTE - 03EGB0023C”, which are funded by the German Federal Ministry for Economic Affairs and Energy (BMWi), and supported by the Lower Saxony Ministry of Science and Culture. The authors are grateful for the support and responsible for the content of the publication.

6. References

- Bertram, E.; Kirchner, M.; Rockendorf, G.; Stegmann, M., (2011), Solarthermie2000plus: Solare Gebäudewärmeversorgung mit unverglasten photovoltaisch-thermischen Kollektoren, Erdsonden und Wärmepumpen für 100% Deckungsanteil. Kurzbezeichnung: BiSolar-WP, Förderkennzeichen: 0325952B.
- Bunea, M.; Perers, B.; Eicher, S.; Hildbrand, C.; Bony, J.; Citherlet, S., (2015), Mathematical modelling of unglazed solar collectors under extreme operating conditions. In: *Solar Energy* 118, S. 547–561. DOI: 10.1016/j.solener.2015.06.012.
- Chhugani, B.; Kirchner, M.; Littwin, M.; Lampe, C.; Giovannetti, F.; Pärish, P., (2020). Investigation of Photovoltaic-Thermal (PVT) collector for direct coupling with Heat Pumps: Hardware in the Loop (HiL) and TRNSYS Simulations. 8th IBPSA Building Simulation Conference for Germany and Austria, BauSim2020.
- Dott, R.; Haller, M. Y.; Ruschenburg, J.; Ochs, F.; Bony, J., (2013), The Reference Framework for System Simulations of the IEA SHC Task 44 / HPP Annex 38. Part B: Buildings and Space Heat Load, A technical report of subtask C Report C1 Part B.
- Giovannetti, F.; Lampe, C.; Kirchner, M.; Littwin, M.; Asenbeck, S.; Fischer, S., (2019). Experimental Investigations on Photovoltaic-Thermal Arrays Designed for the Use as Heat Pump Source. IEA SHC International Conference on Solar Heating and Cooling for Buildings and Industry, Santiago, Chile.
- Haller, M. Y.; Dott, R.; Ruschenburg, J.; Ochs, F.; Bony, J., (2013), The Reference Framework for System Simulations of the IEA SHC Task 44 / HPP Annex 38. Part B: Buildings and Space Heat Load, A technical report of subtask C Report C1 Part A.
- Hüsing, F.; Mercker, O.; Hirsch, H., (2018), Erdwärmekollektoren und Sonnenkollektoren als optimierte bivalente Quelle für hocheffiziente Wärmepumpensysteme. Kurzbezeichnung: „Terra-Solar-Quelle“, Förderkennzeichen: 03ET1275.
- Lämmle, M., (2018), Thermisches Management PVT Kollektoren. Dissertation: Development and modelling of highly efficient glazed, flat plate PVT collectors with low-emissivity coatings and overheating protection.
- Lampe, C.; Kirchner, M.; Littwin, M.; Giovannetti, F.; Asenbeck, S.; Fischer, S., (2019), Experimentelle Untersuchungen an Testfeldern mit SOLINK-photovoltaisch-thermischen Kollektoren. Symposium Solarthermie und Innovative Wärmesysteme, 21-23 May 2019. Bad Staffelstein, Germany.
- Littwin, M.; Chhugani, B.; Lampe, C.; Kirchner, M.; Giovannetti, F.; Pärish, P., (2019), PVT-Systeme: Hardware-in-the-loop Tests und TRNSYS Jahressimulationen. Online Symposium Solarthermie und Innovative Wärmesysteme, 12-14 May 2020. Bad Staffelstein, Germany.
- Leibfried, U.; Wagner, A.; Abdul-Zahra, A., (2017), Hocheffiziente, auf intelligenter Verknüpfung von PVT- und Wärmepumpentechnik basierende Wärmeversorgung für Gebäudebestand und Neubau. Schlussbericht zum Förderprojekt SOLINK, Aktenzeichen: 33226/01.
- Malenković, I.; Pärish, P.; Eicher, S.; Bony, J.; Hartl, M., (2012), Definition of Main System Boundaries and Performance Figures for Reporting on SHP Systems, Deliverable B1, IEA SHC Task 44/ HPP Annex 38.